JPET Fast Forward. Published on January 26, 2007 as DOI: 10.1124/jpet.106.118265
JPET #118265

Preclinical Pharmacokinetic and Pharmacodynamic Evaluation of Metronomic and Conventional Temozolomide Dosing Regimens

Qingyu Zhou, Ping Guo, Xiaomin Wang, Silpa Nuthalapati, James M Gallo

Department of Pharmaceutical Sciences, School of Pharmacy, Temple University, 3307 North Broad Street, Philadelphia, PA 19140.

JPET Fast Forward. Published on January 26, 2007 as DOI: 10.1124/jpet.106.118265
This article has not been copyedited and formatted. The final version may differ from this version.

Running Title: PK/PD study of metronomic and conventional temozolomide doing

Corresponding author:

James M. Gallo, Ph.D.

Department of Pharmaceutical Sciences, School of Pharmacy, Temple University, 3307 North Broad Street, Philadelphia, PA 19140; Phone: 215-707-9699; Fax: 215-707-9409; E-mail: jmgallo@temple.edu

Number of text pages: 41

Number of figures: 6

Number of tables: 2

Number of references: 40

Number of words: 250 in Abstract

733 in Introduction

1467 in Discussion

Abbreviations: MD, metronomic dosed; CD, conventional dosed; PK, pharmacokinetic; PD, pharmacodynamic; TMZ, temozolomide; IF, interstitial fluid; IFP, interstitial fluid pressure; CNS, central nervous system; BBB, blood-brain barrier; MTIC, 3-methyl-(triazen-1-yl)imidazole-4-carboxamide; AIC, 5(4)-aminomidazole-4(5)-carboxamide; O^6MeG, O^6-methylguanine; MGMT, O^6-methylguanine-DNA methyltransferase; MTD, maximum tolerated dose; bFGF, basic fibroblast growth factor; VEGF, vascular endothelial growth factor; GBM, glioblastoma multiforme; HIF-1α; hypoxia inducible factor-1α; Ang-1; angiopoietin 1; Ang-2, angiopoietin 2; TSP-1, thrombospondin-1; HUVEC, Human umbilical vein endothelial cells; DMEM, Dulbecco's Modified Eagle Medium; FBS, fetal bovine serum; PAC, paclitaxel; IV,

intravenous; LC/MS/MS, liquid chromatography/mass spectrometry/mass spectrometry; PCR; polymerase chain reaction; cDNA, complementary DNA; C_T, threshold cycle number.

Preferred section: Chemotherapy, Antibiotics, and Gene Therapy

Abstract

Metronomic dosed (MD) chemotherapy as opposed to conventional dosed (CD) chemotherapy is considered an alternate strategy to target angiogenesis and limit host toxicity. Although promising, there has not been any attempt to define optimal metronomic dosing regimens by integrating pharmacokinetic (PK) with pharmacodynamic (PD) measurements. This study was aimed at comparing the PK and PD of temozolomide (TMZ) following MD and CD regimens. *In vivo* studies were carried out in xenografted athymic rats treated with either 18 mg/kg/d TMZ for 5 days or 3.23 mg/kg/d TMZ for 28 days. PK studies were performed on the first and last days of dosing. PD measurements consisted of gene and protein expression of various angiogenic markers, tumor size, tumor pH and interstitial fluid pressure (IFP). The results demonstrated that the PK parameters (total clearance, volume of distribution, tumor/plasma accumulation) were quite similar for MD and CD groups, consistent with the linear PK properties of TMZ. Both TMZ treatment schedules caused a significant decrease in interstitial fluid pressure (IFP) and tumor size compared to vehicle control treatment, demonstrating a comparable effectiveness of MD and CD regimens. Using real-time PCR and Western blot analyses, some differences were noted in expression levels of VEGF and HIF-1α suggesting that the MD regimen may be superior to the CD regimen by preventing tumors from progressing towards a proangiogenic state. In conclusion, several PK/PD factors contributing to the antitumor activity of the MD TMZ therapy have been identified, and form a foundation for further investigations of low-dose TMZ regimens.

Introduction

Gliomas represent the most common and aggressive type of primary brain tumors, accounting for 42% of all primary nervous system (CNS) tumors and 77% of all malignant primary CNS tumors (Ashby and Ryken, 2006). Despite advances in the multidisciplinary approach and diagnostic imaging techniques, the overall prognosis for patients with high-grade malignant gliomas still remains bleak, with a median survival measured in months, and an overall 5-year survival rate of 2% or less (Surawicz et al., 1998). In the past, the chemotherapeutic approach to malignant brain tumors mainly relied on the use of nitrosoureas, which showed only modest antitumor activity (Nieder et al., 2000). More recently, TMZ has emerged as a well-tolerated oral alkylating agent that is able to cross the blood-brain barrier (BBB) with demonstrated encouraging activity in primary and recurrent gliomas (Newlands et al., 1992; Dehdashti et al., 2006).

TMZ (8-carbamoyl-3-methylidazo(5,1-D)-1,2,3,5-terrazin-4(3H)-one) is rapidly and well absorbed after oral administration (Stevens et al., 1987; Newlands et al., 1992), and undergoes spontaneous hydrolysis at physiological pH to form its active metabolite, 3-methyl-(triazen-1-yl)imidazole-4-carboxamide (MTIC), which further degrades to 5(4)-aminomidazole-4(5)-carboxamide (AIC) and a highly reactive methyl-diazonium cation (Stevens et al., 1987; Denny et al., 1994). MTIC exerts its cytotoxic effect primarily through methylation of genomic DNA at the O^6 position of guanine. The formation of O^6-methylguanine (O^6MeG) subsequently induces futile cycling of a mismatch repair pathway, leading to inhibition of DNA replication and cell-cycle arrest at the G2-M phase transition (Denny et al., 1994; Roos et al., 2007). The O^6MeG

lesion can be repaired by cellular O^6-methylguanine-DNA methyltransferase (MGMT), which transfers the methyl group to a cysteine residue (Trivedi et al., 2005).

The standard recommended dose of TMZ as a single agent or in combination is 150-200 mg/m^2 daily for 5 consecutive days repeated every 4 weeks (Brandes et al., 2002). Other administration schedules, including compressed and extended dosing protocols, being evaluated with the intention of maximizing MGMT depletion, and hence, potentiating the cytotoxicity have demonstrated limited improvement of clinical efficacy with potentially increased hematological toxicity (Danson et al., 2003; Tosoni et al., 2006). Thus, there is a need to reappraise the dose and schedule of TMZ to further improve its effectiveness while reducing its toxicity.

Metronomic chemotherapy, which refers to the frequent administration of chemotherapeutics at doses significantly below the maximum tolerated dose (MTD) without prolonged drug-free breaks, has been evaluated as an alternative strategy to achieve long-term therapeutic control (Gasparini 2001; Kerbel and Kamen 2004). The primary mechanism for metronomic chemotherapy is thought to be due to inhibition of tumor angiogenesis by direct killing of endothelial cells in the tumor neovasculature (Miller et al., 2001), and suppressing the mobilization and levels of bone marrow derived circulating endothelial progenitor cells (Bertolini et al., 2003). As such, metronomic chemotherapy may possess several advantages over conventional chemotherapy, including delaying the onset of acquired drug resistance and reducing host toxicity. Two milestone studies by Browder et al. (2000) and by Klement et al.(2000) followed by several subsequent studies have illustrated the capacity of different cytotoxic agents to preferably target the endothelial cell compartment of tumors when lower doses were given more frequently (Shaked et al., 2005; Klink et al., 2006)

Several studies have been carried out to assess the antiangiogenic potential of the protracted low-dose TMZ treatment. An early preclinical study demonstrated that angiogenesis was inhibited by 5 μM of TMZ in both chorloallantoic membrane and human umbilical vein endothelial cell (HUVEC)-based Matrigel assays (Kurzen et al., 2003). A recent clinical study showed that after receiving continuous low-dose TMZ plus rofecoxib treatment, patients harboring highly angiogenic glioblastoma multiforme (GBM) had a significantly longer time to progression compared with patients with low angiogenic GBMs (Tuettenberg et al., 2005), which suggested an antiangiogenic activity for continuous low-dose TMZ plus rofecoxib. A more recent preclinical study demonstrated that metronomic treatment with TMZ exerted both antiangiogenic and antitumor effects in a TMZ-resistant C6/LacZ rat glioma model (Kim et al., 2006).

Although previous studies showed that TMZ might possess potential antiangiogenic properties when given metronomically, further investigation is warranted to understand PK-PD relationships that can guide the selection of optimal metronomic dosing regimens of TMZ. Therefore, the aim of the present study was to characterize and contrast the pharmacokinetics and pharmacodynamics of TMZ in nude rats with human glioma xenografts receiving either CD or MD TMZ treatment, and in so doing, provide a foundation for the design of optimal MD TMZ treatments.

Material and Methods

Materials

TMZ was generously provided by Schering-Plough Research Institute (Kenilworth, NJ). Paclitaxel (PAC), protease inhibitor cocktail and a mouse monoclonal anti-angiopoietin 1 (Ang-1) antibody were purchased from Sigma-Aldrich Company (St. Louis, MO). Rabbit polyclonal anti-vascular endothelial growth factor (VEGF), anti-hypoxia inducible factor-1α (HIF-1α), anti-Tie-2 antibodies and a goat polyclonal anti-Ang-2 antibody were purchased from Santa Cruz Biotechnology (Santa Cruz, CA). A mouse monoclonal anti-thrombospondin-1 (TSP-1) antibody was from NeoMarkers (Fremont, CA). Matrigel was from Becton-Dickinson (Bedford, MA). HUVECs and the HUVEC media-kit, EGM-2 BulletKit, were from Cambrex Bio Science (Walkersville, MD). Dulbecco's Modified Eagle Medium (DMEM) was from Mediatech, Inc. (Herndon, VA). Fetal bovine serum (FBS) and Trizol® reagent was purchased from Invitrogen (Carlsbad, CA). A protein assay kit was obtained from Bio-Rad (Hercules, CA). Chemiluminescence reagent *plus* was from PerkinElmer (Boston, MA). All other chemicals and solvents were obtained from commercial sources.

Drug analyses were conducted on an API 4000 triple quadrupole liquid chromatography/mass spectrometry/mass spectrometry (LC/MS/MS) system (Applied Biosystems, Foster City, CA). Microdialysis apparatus including microdialysis probes (CMA/20) with a 20 kDa mol wt. cut-off polycarbonate dialysis membrane, a microdialysis pump (CMA/102) and a refrigerated fraction collector (CMA/170) were purchased from CMA Microdialysis (North Chelmsford, MA).

Male athymic nude rats (rnu/rnu) were purchased from Taconic Farms (Germantown, NY) and used for xenografting at the age of 6-7 weeks. The care and use of animals was approved by the Institutional Animal Care and Use Committee in accordance with National Institutes of Health guidelines.

Cell Culture and *In Vitro* Cytotoxicity Assay

HUVECs were cultured in EGM-2 Bulletkit composed of endothelial cell basal medium-2 (EBM-2 medium) supplemented with ascorbic acid, FBS, hydrocortisone, FGF, VEGF, human epidermal growth factor, long R insulin-like growth factor-1, gentamicin sulfate and heparin as described by the manufacturer. A human SF188 glioma cell line that was transfected with the mouse full-length $VEGF_{164}$ cDNA as reported previously (Ma et al., 1998) and thereby overexpressing VEGF (V+) were grown in DMEM supplemented with 10% standard FBS. Cells were maintained in a humidified atmosphere of 5% CO_2 in air at 37^{o}C.

For the i*n vitro* cytotoxicity study, 24-h and 144-h exposures to TMZ and PAC in HUVECs and SF188V+ cells were compared. Cells were seeded in 96-well plates and allowed to attach overnight, and then treated with TMZ and PAC at various concentrations for 24 h (2×10^3 cells/well in 100 μl of medium) or for 144 h (500 cells/well in 100 μl of medium). During the 144-h treatment period, culture media were changed every 24 h along with fresh drug solutions. At the end of the treatment, cells were fixed with trichloracetic acid and stained with sulforhodamine B. Optical densities were measured at 570 nm with a SpectraMax M2 microplate reader equipped with SoftMax Pro software (Molecular Devices, Sunnyvale, CA). The growth of treated cells was expressed as a percentage of control cultures (vehicle alone). The concentration of drugs that decreased the number of viable cells by 50% (i.e., IC_{50}) as compared

to untreated cells was calculated by nonlinear fitting of the experimental data obtained from 3 independent experiments performed in quadruplicate.

Xenografts and *In Vivo* Study Protocol

SF188V+ tumor cells at logarithmic growth *in vitro* were harvested and washed twice with phosphate-buffered saline. Tumor cells (5×10^6) suspended in 0.3 ml Matrigel were inoculated subcutaneously in the dorsal neck region of the athymic rats (6-7 weeks old male rats) through a 23-gauge needle. Tumor growth was monitored twice a week. Two perpendicular diameters (*a* and *b*) were measured with a vernier caliper (Fisher Scientific, Newark, DE), and tumor volumes (*V*) were calculated using the following formula: $V = 0.5ab^2$ (Kato et al., 1994). At a tumor size of ~ $1cm^3$, nude rats were randomized into three groups: (1) the vehicle control group (daily intravenous (IV) administration of 25% DMSO in saline), (2) the CD group (daily IV administration of TMZ for 5 days at a dose of 18 mg/kg by a 10-min infusion at a rate of 2 mg/kg/min), and (3) the MD group (daily IV bolus injection of TMZ for up to 28 days at a dose of 3.23 mg/kg/d). The dosing regimen of TMZ for the CD group is equivalent to the TMZ dose of 200 $mg/m^2/d$ for 5 days used clinically based on the reported formula of conversion between rat body weight and surface area (Freireich et al., 1966). A course of MD TMZ treatment consisted of daily administration of 3.23 mg/kg TMZ for 28 days, which corresponded to a cumulative dose of 90 mg/kg and was equivalent to the total of the five daily treatments of 18 mg/kg of TMZ of the CD regimen. On days 5, 14 and 28, a subgroup of rats from each group was euthanized with CO_2 and the tumor mass was excised. The tumor was dissected using a razor blade and snap frozen in liquid nitrogen and then stored at -80^oC before total RNA

extraction and tissue lysate preparation. Body weights and tumor volumes were measured twice a week throughout the experiment.

Measurement of Tumor pH and IFP

Tumor pH and IFP in both the central and peripheral region of the tumor were measured one day before the initiation of both CD or MD TMZ treatment, and once a week thereafter. The extracellular pH of tumor tissue was measured by inserting a small needle probe connected to a pH meter (Jenco Electronics Ltd., San Diego, CA) into the tumor. The measurement of IFP was performed using the "wick-in-needle" technique that also entailed the placement of a small probe connected to a pressure transducer (Kent Scientific Co., Torrington, CT) into the tumor (Fadnes et al., 1977).

PK Blood Sampling and Tumor Microdialysis Study

One day before the initiation of TMZ treatment, a right femoral vein and femoral artery were surgically catheterized for drug administration and blood sampling, respectively. The pharmacokinetics of TMZ was assessed in two separate groups of 7 – 9 rats, which were given either daily IV administration of 18 mg/kg TMZ by a 10-min infusion at a rate of 2 mg/kg/min for 5 days (the CD group) or daily IV bolus injection of 3.23 mg/kg TMZ for 28 days (the MD group). PK blood sampling periods were on both the first and last days (day 5 and day 28 for CD and MD groups, respectively) of dosing with 100 μl blood samples collected from each rat at pre-dose, 5, 10, 20 and 40 min, 1, 1.5, 2, 3, 4, 5, 6, and 8 h after the start of drug administration. The blood samples were immediately centrifuged and 50 μl of plasma was acidified with 10 μl of 0.1% formic acid and added to 100 μl of acetonitrile to precipitate proteins. Following

centrifugation at 14,000 rpm for 5 min, the supernatant was collected and stored at -80 ^{o}C until analysis.

On the day of the experiment, CMA/20 dialysis probes with a membrane length of 10 mm were inserted into the central region of the tumor. Prior to the administration of TMZ, the probes were perfused at a rate of 2 μl/min with Ringer's solution (147 mM NaCl, 2.3 mM $CaCl_2$, 4.0 mM KCl) containing 200 ng/ml of TMZ. After a 45-min equilibration period, microdialysate samples were collected automatically with a CMA/170 refrigerated fraction collector for 40 min in fractions corresponding to 10-min intervals. The *in vivo* recovery determined from the loss of TMZ from the perfusate was calculated for each interval of time according to the following equation (Wang et al., 1993):

$$RR = \frac{C_{in} - C_{out}}{C_{in}}$$

where *RR* is the *in vivo* relative recovery, C_{in} is the drug concentration in perfusate, and C_{out} is the drug concentration in microdialysate. The mean *RR* value obtained from four individual determinations was used as the *in vivo* recovery to correct the dialysate concentrations that allowed unbound TMZ concentrations in the interstitial fluid to be calculated as the concentrations in the microdialysate divided by the mean *RR*.

Following the calibration period for the microdialysis probes, a washout period of 40 min with blank Ringer's solution perfusion was allowed prior to IV TMZ administration. Microdialysate samples were collected at 10-min intervals for 6 hours after TMZ administration at a flow rate of 2 μl/min, and then stored at -80 ^{o}C until analysis.

Drug Analysis

TMZ concentrations in the plasma and tumor microdialysate were quantitated using electrospray ionization LC/MS/MS. Briefly, the plasma sample (50 μL) with the addition of the internal standard dacarbazine (8 ng/ml)) was deproteinized with acetonitrile containing 0.1% formic acid (100 μL). After centrifugation (14,000 rpm × 10 min), an aliquot of 7 μL of the supernatant was injected into the LC/MS/MS system. An aliquot of 15 μL of tumor microdialysate spiked with the internal standard (17 ng/ml) was directly injected into the LC/MS/MS system. The LC system consisted of a C18 guard cartridge (4.0 × 2.0 mm, Phenomenex, Torrance, CA) and a Luna C18 analytical column (Phenomenex, 50 × 2.0 mm, 3 μm particle size) with an isocratic mobile phase consisting of acetonitrile:0.5 mM ammonium formate containing 0.1% formic acid (8:92 and 4:96, v/v, for plasma and microdialysate samples, respectively). The flow rate was 0.2 ml/min. The column temperature was maintained at 35 ºC. The instrument was operated in the positive ion scan mode, monitoring the ion transitions from m/z 195.1→137.9 for TMZ and m/z 183.2→123.3 for dacarbazine (the internal standard) with a dwell time of 800 ms for each ion transition. The low limit of quantification was 9 and 8 ng/ml for TMZ in plasma and tumor microdialysate, respectively. The mean extraction recovery of TMZ was 103.6% and 94.8% for plasma and tumor microdialysate, respectively. The intra- and inter-assay precisions determined over a concentration range of 9 to 43500 ng/ml for plasma and 8 to 12569 ng/ml for microdialysate were all less than 15%, and the accuracy expressed as the percentage error was within the range of ± 15% and ± 20% for plasma and tumor microdialysate, respectively.

PK Analysis

JPET Fast Forward. Published on January 26, 2007 as DOI: 10.1124/jpet.106.118265
This article has not been copyedited and formatted. The final version may differ from this version.

PK data analyses were performed using the software package SAAM II (version 1.0B, University of Washington, Seattle, WA). A hybrid PK model that consisted of a forcing function describing the plasma concentration-time profile and a 1-compartment tumor model was used to characterize drug disposition in plasma and tumor tissue (Fig. 1). Parameters estimated in the model included the volume of distribution (V_p), the elimination rate constant (K_e), the intercompartmental rate constants (i.e., K_{pt} and K_{tp}), and the area under the plasma or tumor IF concentration-time curve ($AUC_{0\rightarrow t,p}$ and $AUC_{0\rightarrow t,t}$ for plasma and tumor IF, respectively) from 0 to the last quantifiable time point. The volume of the tumor compartment (V_t) was fixed at the actual tumor volume measured in individual animals on the day of PK sampling. PK parameters calculated from these estimates included systemic clearance (CL_p), and the total area under the concentration-time curves ($AUC_{0\rightarrow\infty}$). The peak plasma concentration (C_{max}) and the peak time (t_{max}) were obtained by visual inspection of the plasma and tumor IF concentration-time curves.

Quantitative Real-Time PCR Assay

One microgram of total RNA extracted from tumor tissues with Trizol reagent was reverse transcribed into complimentary DNA (cDNA) using random hexamer primers and AMV reverse transcription reagents as per the manufacturer's protocol (Promega, Madison, WI). Then, 50 ng of cDNA was subject to quantitative real-time PCR for the selected genes, i.e., human *VEGF*, rat *HIF-1α*, rat *TSP-1*, rat *Ang-1*, rat *Ang-2*, rat *Tie-2* and human *β-actin* (the endogenous control), using the pre-developed 20× TaqMan® gene expression assay mix (assay identification numbers are Hs00173626_m1, Rn00577560_m1, Rn00449032_g1, Rn00585552_m1, Rn01756774_m1, Rn01433337_m1 and Hs99999903_m1 for human *VEGF*, rat *HIF-1α*, rat *TSP-1*, rat *Ang-1*, rat *Ang-2*, rat *Tie-2* and human *β-actin*, respectively. Applied Biosystems, Foster City, CA).

JPET Fast Forward. Published on January 26, 2007 as DOI: 10.1124/jpet.106.118265
This article has not been copyedited and formatted. The final version may differ from this version.

Polymerase chain reaction (PCR) amplification was performed on 2 μl of cDNA template in a 25-μl reaction mixture containing 12.5 μl of TaqMan® universal PCR master mix, 1.25 μl TaqMan® gene expression assay mix (Applied Biosystems, Foster City, CA), and 9.25 μl of RNase-free water. During the extension phase of PCR, the nucleolytic DNA polymerase cleaved the hybridization probe, and the resulting relative increase in the reporter fluorescent dye emission was monitored in real time using an Applied Biosystems 7300 real-time PCR system (Applied Biosystems, Foster City, CA). The fluorescent dye emission was a function of cycle number and was determined using the sequence detection software (Applied Biosystems), giving the threshold cycle number (C_T) at which the increase in normalized fluorescence over a defined threshold that first occurs for each amplification plot. Each RNA sample was tested in quadruplicate, and the C_T values were averaged. The relative amounts of the six genes were calculated by means of the $\Delta\Delta C_T$ method. Briefly, the arithmetic formula for the $\Delta\Delta C_T$ method is given by $2^{-\Delta\Delta C_T}$, where ΔC_T is the C_T value of each target gene minus the C_T value of the *β-actin*, which gives a normalized value. The $\Delta\Delta C_T$ was obtained by subtracting the normalized ΔC_T value of each target gene from the normalized ΔC_T value of a calibrator, which was a tumor sample obtained from an untreated rat (neither vehicle nor TMZ). The formula $2^{-\Delta\Delta C_T}$ therefore gives a relative value when comparing the target to the calibrator.

Western Blot Analysis

Tumor tissues were homogenized in 1ml cell lysis buffer (50 mM Tris-HCl (pH 7.5), 137 mM NaCl, 10% glycerol, 1% NP-40, 2mM EDTA, 25 mM β-glycerophosphate, 50 mM NaF, 10 mM NaPPi, 1 mM Na_3VO_4 and protease inhibitor cocktail) per 200 μg of frozen tissue. Lysis was carried out at 4^oC for 30 minutes and lysates were centrifuged at 15,000 rpm for 20 minutes.

JPET Fast Forward. Published on January 26, 2007 as DOI: 10.1124/jpet.106.118265
This article has not been copyedited and formatted. The final version may differ from this version.

The protein concentration of the supernatant was determined using the Bio-Rad Protein Assay (Bio-Rad, Hercules, CA). Equal amounts (70 μg) of proteins were separated on pre-cast sodium dodecyl sulfate-polyacrylamide gels (Life Therapeutics, Frenchs Forest, Australia) and transferred to PVDF membranes. After being blocked in Tris-buffered saline with 0.1% Tween-20 containing 5% nonfat milk, the membranes were immunoblotted overnight at 4^{o}C with the following antibodies: VEGF (1:400), HIF-1α (1:400), TSP-1 (1:400), Ang-1 (1:400), Ang-2 (1:200) and Tie-2 (1:400). Blots were incubated with horseradish peroxidase–conjugated secondary antibodies (1:15,000; Santa Cruz Biotechnology) at room temperature for 1 hour and immunoreactive protein bands were visualized by the enhanced chemiluminescence system (PerkinElmer). The membranes were then stripped and reprobed with β-actin (1:4000) to ensure equal protein loading. Band areas were quantified by ImageJ software (from NIH and available at http://rsb.info.nih.gov/ij/). The expression levels of individual proteins are presented as fold changes when compared with the non-treated control (i.e. the same tumor sample used as the calibrator for the real-time PCR).

Statistical Analysis

Data analyses were performed using Number Cruncher Statistical Systems 2004 (Keysville, UT). The evaluation of differences in medians between two related samples and between two independent groups was made using Wilcoxon signed-rank test and Wilcoxon rank-sum test, respectively. The evaluation of differences in means between two independent groups was made using the equal-variance *t*-test. In case of multiple comparisons, Kruskal-Wallis one-way analysis of variance on ranks was used. Pearson correlations were used to describe relations

between two variables. A two sided P-value of less than 0.05 was considered statistically significant.

Results

In Vitro Cytotoxicity of TMZ in HUVEC and SF188V+ Cells

The therapeutic action of anticancer drugs may be attributed to toxicity to both proliferating endothelial cells and tumor cells (Gasparini 2001; Hahnfeldt et al., 2003). Based on the previous observations that various cytotoxic drugs acted preferentially on endothelial cells when the cells were exposed to the individual drugs daily for up to 6 days (Bocci et al., 2002), we contrasted the *in vitro* cytotoxicity of protracted TMZ exposure for 144 h to the relatively short TMZ exposure for 24 h in HUVECs and SF188V+ human glioma cells to determine whether MD TMZ treatment could have the same propensity to inhibit endothelial cell growth. PAC, which has consistently shown preferential antiproliferative activity against endothelial cells when given at low doses in a continuous manner, served as a positive control in this study (Bocci et al., 2002). In addition, standard culture conditions were used in this study to mimic certain aspects of the *in vivo* tumor microenvironment by adding several proangiogenic growth factors in the culture medium. When SF188V+ glioma cells and HUVECs were exposed to TMZ or PAC for only 24 h, both drugs displayed moderate or mild cytotoxic properties with the IC_{50} values being greater than 1 mM for TMZ in both cell lines, whereas for PAC the IC_{50} was 1.79 nM and > 3 μM in SF188V+ cells and HUVECs, respectively (Fig. 2). In sharp contrast, protracted low-dose TMZ and PAC treatment for 144 h significantly inhibited the growth of SF188V+ cells and HUVECs at relatively low concentrations compared with the 24-h treatment. The IC_{50} values for SF188V+ cells and HUVECs in the 144-h TMZ treatment were about 48- and 39-fold lower, respectively, than those in the 24-h treatment ($P < 0.01$). Likewise, the IC_{50} value for SF188V+ cells in the 144-h PAC treatment was 2.6-fold less than that in the 24-h treatment ($P < 0.01$).

Notably, the cytotoxicity of TMZ appeared to be more pronounced against SF188 V+ cells than HUVECs (IC_{50} of 24.0 ± 0.51 μM *versus* 35.8 ± 1.15 μM, $P < 0.01$). In contrast, the control drug PAC was in agreement with the literature (Bocci et al, 2002), showing a more potent cytotoxic effect on HUVECs than on SF188V+ cells (IC_{50} of 0.680 ± 0.048 nM *versus* 0.288 ± 0.037 nM, $P < 0.01$).

Systemic and Tumor Distribution of TMZ in Tumor-Bearing Athymic Rats

The PK study was designed to compare the disposition of TMZ in plasma and tumors following CD and MD regimens, which would enable an assessment of both dose-dependent and time-dependent alterations in TMZ's PK properties. The plasma pharmacokinetics of TMZ is known to be linear and reproducible within and between patients (Newlands et al., 1992). However, there is minimal information on the accumulation of TMZ within tumors (Ma et al., 2001, 2003), regardless of the dosing regimen. In consideration of using MD TMZ with anticipated antitumor and/or antiangiogenic activity, it was of interest to compare its distribution into tumor to that obtained with CD TMZ. For this purpose, microdialysis was utilized so that interstitial fluid unbound drug concentrations could be measured, this extravascular sampling compartment being adjacent to both tumor and endothelial cells.

Seven rats from the CD group and 9 from the MD group had complete PK studies performed on the 1st day and the last day of treatment. A compartmental modeling analysis applied to individual rats in CD and MD groups revealed that for some animals the best fit of plasma concentration data was achieved with a one-compartment model, while a two-compartment model provided the best fit for the others. Once the best-fit compartment model was defined for each animal from the TMZ's plasma-time profile, it was set as a forcing function in the

JPET Fast Forward. Published on January 26, 2007 as DOI: 10.1124/jpet.106.118265
This article has not been copyedited and formatted. The final version may differ from this version.

compartment model that was fit to the corresponding TMZ tumor concentrations (Fig. 1). Definition of a constant forcing function in the development of the tumor models minimized the number of parameters that had to be estimated. The PK data for TMZ at each dosing regimen is summarized in Table 1, with mean plasma and tumor interstitial fluid (IF) TMZ concentration time profiles as well as the representative predicted and observed plasma and tumor IF concentrations shown in Fig. 3A-3D. Compartmental model predicted TMZ concentrations in both plasma and tumor IF showed remarkably good agreement between predicted and observed values (Fig. 3C and 3D). The pharmacokinetics of TMZ appeared linear, both dose- and time-independent, since there were no differences between the systemic clearance and volume of distribution in the CD and MD groups on day 1 and the last treatment day. Within each type of TMZ dosing schedule, these parameters remained essentially constant on day 1 and day 5 in the CD group, and on day 1 and day 28 in the CD group. The ratio of the mean $AUC_{0\rightarrow\infty,p}$ values on day 1 in the CD group to those in the MD group was 5.6, which was identical to the dose ratio of 5.6 for the CD to MD groups. In addition, as expected from the systemic clearance and volume of distribution values, the $t_{1/2}$ of TMZ remained essentially the same at about 0.9 h, independent of the dose (CD and MD groups), and time (1st day and the last day of treatment).

The analyses of the pharmacokinetics of TMZ in tumor indicated similar trends as in plasma based on CD and MD doses and study days with the exception of the more rapid distribution to the tumor tissue (K_{pt}) in the MD group compared to that in the CD group (6.77 versus 2.69; $P < 0.01$) on the last day of treatment (Table 1). There was no significant difference in the time of peak tumor concentrations between the CD and MD groups. The unbound TMZ concentrations in tumor decreased rapidly thereafter with the $t_{1/2}$ values similar to those determined in plasma and ranged from a mean of 0.99 h to 1.28 h. The CD-to-MD day 1 ratios of both C_{max} and

JPET Fast Forward. Published on January 26, 2007 as DOI: 10.1124/jpet.106.118265
This article has not been copyedited and formatted. The final version may differ from this version.

AUC_{tumor} values were 2.2 and 3.2, respectively, and less than that anticipated from the dose ratio of 5.6. This potential nonlinear phenomenon was not observed on the last treatment days (day 5 and day 28) when the $C_{max,t}$ and $AUC_{0\rightarrow\infty,t}$ ratios were 5.5 and 6.7, respectively, analogous to the dose ratio of 5.6. The lower than expected ratios of C_{max} and AUC_{tumor} on day 1 could be attributed to the day 1 TMZ measurements in the MD treatment group in which TMZ concentrations were higher than those obtained on day 28. These high TMZ measurements also translated into higher than expected mean AUC_{tumor} /AUC_{plasma} ratios in the MD group on day 1, being 1.7-fold higher than that in the CD group although the difference was not statistically significant ($P > 0.05$). However, on the last day of treatment (day 5 for CD and day 28 for MD), the mean AUC_{tumor} /AUC_{plasma} ratios were analogous at a mean of 1.25. In considering TMZ PK data over the complete treatment periods, there were no sustainable changes in tumor accumulation between the CD and MD regimens, consistent with the relatively short half-life (~ 0.9 h) and linear PK behavior of the drug.

Toxicity

Since there were no animal deaths in this study, animal weight loss was used as an indicator of toxicity associated with either the CD or MD TMZ treatment. One week after the start of the treatment, weight loss was observed in treated animals, but it was only 9% and 6% for the CD and MD groups, respectively. The weights of animals receiving both CD and MD TMZ treatments were regained by the end of the 28-day study period. An analysis of variance showed a lack of statistically significant differences in body weight between control and TMZ treatment groups prior to and during the period of treatment ($P > 0.05$). Except for suppressing body

weight gain in rats, no other systemic toxicity related to the MD TMZ treatment was observed, demonstrating that the MD regimen applied in this study is well-tolerated in the rat model.

Effect of TMZ on SF188 V+ Tumor Growth, Tumor pH and IFP in Nude Rats

Tumor size is the most common parameter used to assess effective anticancer treatment in preclinical models. Although considered a crude endpoint, it is important to include its measurement with the hope to identify correlations to PK/PD measurements that could serve as the basis to design drug dosing regimens. As expected, SF188V+ xenografts grew progressively in the vehicle control animals with a 3-fold increase in the mean tumor volume by day 28 ($P < 0.01$, Fig. 4A). In contrast, tumors treated with either CD or MD TMZ approached a highly significant delay in tumor growth as compared with the control with the maximum tumor growth inhibition of 71% and 49% for the CD and MD group, respectively ($P < 0.01$) (Fig 4A). Notably, tumor growth delay in the CD group persisted for up to 3 weeks after the cessation of the treatment. In addition, there was no statistical difference in tumor size between CD and MD groups.

Tumor IFP is used as an indicator of vascular integrity and hypoxia, and often shows regional variations within the tumor (Jain 1987). Large tumors containing regions of hypoxia will possess higher IFP than smaller well-perfused tumors. These types of changes can influence macromolecular and small molecular weight drug transport by convection. Consistent with that expectation for large untreated tumors, we found IFP was significantly increased in the control group on day 21 and 28 irrespective of the region of the tumor ($P < 0.01$ for both). Both CD and MD TMZ treatments produced a significant decrease in IFP in both central and peripheral regions of the tumor compared to the control from day 7 through day 28 (Fig. 4B). These data

support the possibility that TMZ could enter tumors by convective transport due to the reduction in IFP.

Tumor cells have a natural tendency to overproduce acids, resulting in very acidic pH values in the extracellular space. This can be further exacerbated by oxygen depletion and nutrient/energy deprivation in large tumors (Vaupel et al., 1989). Consistent with these findings, our data showed that tumor pH in the control group tended to decline as the tumor volume increased regardless of the region of the tumor, and on day 28, a statistically significant decrease in tumor pH was observed in the central region of tumors ($P < 0.05$), while a trend towards lower pH values was found for the peripheral region ($P = 0.069$) (Fig. 4C). Tumor pH may affect the formation of MTIC, which usually results from the spontaneous hydrolysis of TMZ at physiological pH (Stevens et al., 1987; Denny et al., 1994). However, we observed that tumor pH in the TMZ treatment groups basically remained unchanged and tended to be greater than in the control groups with the only significant difference found on day 28 whereby tumor pH was greater (mean values about 7.15) in the MD group, but not in the CD group compared to control. In this regard, the effect of tumor pH on the cytotoxicity of TMZ related to the formation of MTIC would be marginal.

Evaluation of mRNA Expression Levels of *VEGF*, *HIF-1α*, *TSP-1*, *Ang-1*, *Ang-2* and *Tie-2* in SF188V+ Xenografts

Tumor-induced angiogenesis is essential for the progression and metastasis of solid tumors. This process involves a diverse array of molecules including those that stimulate endothelial cell proliferation and migration as well as those that regulate the maintenance and destruction of the perivascular milieu. To characterize the angiogenic-related molecular and cellular responses that

occur after the CD and MD TMZ treatment, we examined changes in expression of several angiogenic mediators, *VEGF*, *HIF-1α*, *TSP-1, Ang-1, Ang-2* and *Tie-2,* in response to the CD and MD regimens using quantitative real-time PCR.

No significant changes in *VEGF* mRNA expression levels were observed in the control group during the experimental period. This could be attributable to the high basal expression level of *VEGF* gene in the SF188V+ cells, which were designed to overexpress VEGF. The observed elevation of the *HIF-1α* gene expression level in the control group on day 5 compared with the basal level is consistent with the anticipation that rapid tumor growth results in oxygen depletion, leading to the upregulation of *HIF-1α* expression; whereas the significantly decreased mRNA expression level of *HIF-1α* by day 28 ($P < 0.05$) would suggest that tumor cells have adapted to survive under conditions of hypoxia. Interestingly, the expression of *VEGF* mRNA was significantly upregulated in both CD and MD groups by day 14 ($P < 0.05$ for both), but fell below the respective median *VEGF* expression levels observed on day 5 by day 28. Similarly, *HIF-1a* gene expression levels in both treatment groups were increased by day 14 and then followed by a significant decrease by day 28 ($P < 0.05$ for both TMZ treatment groups) (Table 2). Significant correlations between *VEGF* and *HIF-1α* gene expression were demonstrated in the correlative plots of $2^{-\Delta\Delta C_T}$ values of *VEGF* (y-axis) versus *HIF-1α* (x-axis) obtained from matched samples, with Pearson correlation coefficients of 0.49 (P=0.018), 0.68 (P=0.003) and 0.84 (P=0.000002) for the control, CD and MD groups, respectively (Fig. 5). This observation is consistent with the expected upregulation of VEGF in response to hypoxia. There was no clear trend in the effect of either CD or MD TMZ treatment on the expression levels of *TSP-1, Ang-1, Ang-2* and *Tie-2* genes in SF188V+ xenografts, and further, no significant correlations were

noted among any other gene expression values in any of the study groups, suggesting multiple mechanisms and pathways are involved in tumor angiogenesis.

Western Blot Analysis

In addition to transcriptional changes in genes associated with selected PD markers of angiogenesis, it was important to also determine protein expression of the same markers since they may not be correlated, and have a different time profile. Since protein expression was monitored at multiple time points during the 28 day study period, the opportunity to identify time-dependent changes in protein induction and inhibition was possible. Semi-quantitative analyses of the expression levels of VEGF and HIF-1α protein were basically in agreement with the real-time PCR data although the fold change in the mRNA expression level was not proportionally reflected at the protein level (Fig. 6A-6C). Western blot analysis showed that VEGF expression levels were slightly increased in the control and CD groups (118.1 ± 33.8% and 122.1 ± 32.2% of the non-treated control, respectively). In contrast, there was a reduction of up to 36% of the basal level of VEGF expression in the MD group with a trend towards significance as compared with the control group on day 28 ($P = 0.066$) (Fig. 6B). A significant up-regulation of HIF-1α expression was observed in the control group on day 5 ($P < 0.05$ and 0.01 compared with the CD and MD groups, respectively), and in the CD group on day 14 ($P< 0.05$ compared with either the same treatment group on day 5 or the MD group on day 14). The expression level of HIF-1α in both CD and MD groups declined significantly on day 28 compared with those in the respective groups on day 14 ($P < 0.05$ and 0.01 for the CD and MD groups, respectively), and a significant difference was also found between the control and MD groups on day 28 (125.8 ± 29.2% versus 87.2 ± 30.5%, $P < 0.05$) (Fig. 6C). Overall, similar to

our real-time PCR findings, the MD regimen appears to maintain better control of angiogenic factors (i.e., avoidance of larger fluctuations) than the CD regimen.

No significant changes in expression of selected angiogenic mediators other than VEGF and HIF-1α were observed among the control and two TMZ treatment groups at any time point (data not shown), suggesting that MD TMZ does not act on any specific pathways mediating angiogenesis like other MD chemotherapeutics, such as cyclophosphamide and PAC (Damber et al., 2006).

Discussion

MD chemotherapy has recently received a great deal of attention as an alternative strategy to conventional MTD regimens for cancer management because it may potentially avoid or at least delay the onset of chemoresistance by targeting tumor vasculature (Gasparini 2001; Kerbel and Kamen 2004). Although recent studies have demonstrated that angiogenesis can be inhibited by low concentrations of TMZ as effectively *in vitro* as *in vivo* (Kurzen et al., 2003; Kim et al., 2006), a better understanding of PK and PD differences between conventional and metronomic TMZ therapy may lead to development of more effective and less toxic therapeutic regimens.

The results of the *in vitro* cytotoxicity assay revealed that the antiproliferative effect of TMZ on both SF188V+ cells and HUVECs was greatly increased when cell proliferation was assessed under protracted treatment conditions in which the drug-containing medium was replaced on a daily basis although the fold changes in the IC_{50} values between the 24-h and 144-h treatment might be exaggerated due to different starting cell concentrations as well as the potentially delayed cytotoxic effect of TMZ. Nonetheless, the results suggest that TMZ is increasingly cytotoxic with increasing time of exposure. An intriguing observation was that extending exposure time increased the antiproliferative potency of TMZ in SF188V+ cells and HUVECs to the same extent, suggesting that the antiproliferative effects of TMZ on both tumor and endothelial cells are essentially identical. The observed statistically significant difference in IC_{50} values between SF188V+ cells and HUVECs however could be due to the faster growth of tumor cells in culture compared with that of endothelial cells as the rates of DNA replication and cell proliferation are known to be essential determinants for TMZ-induced O^6MeG-triggered cell killing (Denny et al., 1994, Roos et al., 2007). Although an early study by Kurzen et al. (2003)

demonstrated that TMZ reduced HUVECs' adhesion to fibronectin and inhibited endothelial cell alignment and cord formation on Matrigel when HUVECs were exposed to TMZ at 5 – 50 μM for 24 h, it could be possible that TMZ's inhibitory effect on endothelial cell functions relevant to angiogenic process was associated with its antiproliferative activity. Therefore, TMZ would have both cytotoxic and antiangiogenic activity *in vivo* at doses which inhibit the proliferation of both tumor and endothelial cells.

A comparison between the *in vivo* drug levels and *in vitro* IC_{50} values for the 144 h-treatment in this study revealed that the *in vivo* tumor IF unbound TMZ concentrations in the CD group were over the IC_{50} values for SF188V+ cells and HUVECs for approximately 3h/day, whereas those in the MD group were far less than the IC_{50} values. However, the effectiveness of MD TMZ was found to be comparable to that of the CD regimen in terms of inhibition of tumor growth and decreased tumor IFP and pH relative to the control group. It was therefore speculated that TMZ might have affected tumor-induced angiogenesis *in vivo* at local concentrations lower than those necessary to cause a cytotoxic effect on tumor cells, and TMZ's antiangiogenic activity at low doses might be attributed to mechanisms other than direct inhibition of endothelial cell proliferation.

To explore whether MD TMZ may exert the *in vivo* tumor suppressive effect through an antiangiogenic mechanism, we investigated the effects of different TMZ dosing regimens on the expression of several cytokines and their receptors that are known to play a pivotal role in tumor angiogenesis. *VEGF* gene expression levels in both CD and MD groups were found to be higher than that in the control group by day 14. A significant correlation between the mRNA expression level of *VEGF* and that of *HIF-1α* suggests that *VEGF* gene expression level is elevated in response to hypoxia. Although no significant changes in VEGF protein expression levels were

observed by the Western blot analyses, the protein expression level of HIF-1α in the CD group was significantly upregulated by day 14, while the HIF-1α protein expression levels in the MD group remained consistent throughout the treatment period, implicating that the effect of TMZ on hypoxia could be dose-related. Although the exact mechanism of the exacerbated hypoxia following TMZ treatment deserves further investigation, the destructive action of TMZ, especially at higher doses, on the tumor vasculature by direct killing of endothelial cells may have caused hypoxia, leading to the initial elevation of *HIF-1α* and *VEGF* gene expression levels. No clear trend could be discerned for the effect of both CD and MD TMZ regimen on the expression of TSP-1, Ang-1, Ang-2 and Tie-2 in this study. Taken together, our results suggest that the antitumor activity of TMZ at either high or low dose levels may be attributed to its antiproliferative activity against both tumor cells and endothelial cells. Nonetheless, unlike the CD treatment that may result in a temporary excessive vascular regression and subsequently exacerbating local hypoxia in tumors, the moderate effect of the MD treatment on tumor endothelial cells may lead to the normalization of tumor vasculature. This in turn could prevent tumors from progressing towards a proangiogenic state that may lead to the enhanced invasiveness of the tumor and an increased possibility of metastatic dissemination (Le et al., 2004).

It is noteworthy in the PK study that, unlike the plasma pharmacokinetics of TMZ that was demonstrated to be linear, both as a function of dose and time, tumor uptake of TMZ was less consistent, and suggested a possible nonlinear phenomenon in the rat model. The mechanisms underlying this potential nonlinear tumor distribution are open to speculation. TMZ is thought not to undergo any specialized membrane transport processes, but to enter and exit cells via passive diffusion due to its high lipophilicity (Bull and Tisdale, 1987). Given an intact tumor

microvascular structure, unbound or protein-free drug is available for diffusion due to a concentration-gradient across the cell membrane. In this case, the tumor interstitial fluid unbound TMZ to total plasma AUC ratios (AUC_{tumor}/AUC_{plasma}) should be on the order of 0.8, which is equivalent to the unbound fraction of TMZ determined in rat plasma (Gallo et al., 2004). However, in this study, this AUC_{tumor}/AUC_{plasma} ratio determined on day 5 in the CD group and those determined on day 1 and day 28 in the MD group were all slightly greater than unity, which raises the question of whether other mechanisms of drug accumulation are involved besides passive diffusion. An alternative explanation for the high TMZ AUC_{tumor}/AUC_{plasma} ratio could be the combined effects of enhanced tumor vascular permeability and reduced IFP found in the TMZ treatment groups (see Fig. 4B), which would enable convective transport to come into play (Jain 1987; Seymour 1992). Convective transport could cause circulating protein-bound and unbound TMZ to extravasate from the compromised tumor vessels leading to higher concentrations of TMZ in tumor IF compared with those attained by diffusional transport alone (Gallo et al., 2004). In the present study, a moderate increase in the protein expression levels of VEGF in TMZ-treated tumors was observed in the first couple of weeks after the start of treatment in the CD group. Overexpression of VEGF may lead to the increase in tumor microvessel permeability, and the increased tumor vascular permeability may have contributed to the significant increase in the AUC_{tumor}/AUC_{plasma} ratio on day 5 compared with those on day 1 in the CD group. In contrast, VEGF expression levels in the MD group were reduced by day 28, which may partially explain the significant decrease in the AUC_{tumor}/AUC_{plasma} ratio in the MD group on day 28. It appears then that early in the TMZ treatments increased microvessel permeability coupled with convective transport elevated TMZ interstitial fluid concentrations; however with continued treatment and abatement of the action of VEGF, the tumor vasculature

may have been normalized (Jain 2005) minimizing convective transport and restoring diffusion as the essential transport mechanism.

In conclusion, we have been able to identify several PK/PD factors that contribute to the antitumor activity of the MD TMZ therapy. The MD TMZ regimen applied in this study exhibits comparable effectiveness to the CD TMZ regimen in suppressing tumor growth most likely by its action on tumor cells, and the collateral antiproliferative activity against endothelial cells of the growing vasculature in tumors. The moderate effect of the MD TMZ therapy on VEGF and HIF-1α expressions in tumors support that the MD regimen may be superior to the CD regimen by normalizing tumor vasculature and preventing tumors from progressing towards a proangiogenic state. In addition, by employing tumor microdialysis drug concentration measurements it is possible to identify a "breakthrough" dose associated with minimal extravacular drug accumulation, which could indicate whether effective MD regimens require accumulation in tumor cells or if endothelial cells alone serve as sufficient targets. Although we have not yet identified a breakthrough MD for TMZ, the current study indicates that TMZ activity as a MD agent requires drug accumulation in tumor cells.

References

Ashby LS and Ryken TC (2006) Management of malignant glioma: steady progress with multimodal approaches. *Neurosurg Focus* **20**:E3.

Bertolini F, Paul S, Mancuso P, Monestiroli S, Gobbi A, Shaked Y and Kerbel RS (2003) Maximum tolerable dose and low-dose metronomic chemotherapy have opposite effects on the mobilization and viability of circulating endothelial progenitor cells. *Cancer Res* **63**:4342-4346.

Bocci G, Nicolaou KC and Kerbel RS (2002). Protracted low-dose effects on human endothelial cell proliferation and survival in vitro reveal a selective antiangiogenic window for various chemotherapeutic drugs. *Cancer Res* **62**:6938-6943.

Brandes AA, Ermani M, Basso U, Paris MK, Lumachi F, Berti F, Amista P, Gardiman M, Iuzzolino P, Turazzi S and Monfardini S (2002) Temozolomide in patients with glioblastoma at second relapse after first line nitrosourea-procarbazine failure: a phase II study. *Oncology* **63**:38-41.

Browder T, Butterfield CE, Kraling BM, Shi B, Marshall B, O'Reilly MS and Folkman J (2000) Antiangiogenic scheduling of chemotherapy improves efficacy against experimental drug-resistant cancer. *Cancer Res* **60**:1878-1886.

Bull VL and Tisdale MJ (1987) Antitumour imidazotetrazines--XVI. Macromolecular alkylation by 3-substituted imidazotetrazinones. *Biochem Pharmacol* **36**:3215-3220.

Damber JE, Vallbo C, Albertsson P, Lennernas B and Norrby K (2006) The anti-tumour effect of low-dose continuous chemotherapy may partly be mediated by thrombospondin. *Cancer Chemother Pharmacol* **58**:354-360.

Danson S, Lorigan P, Arance A, Clamp A, Ranson M, Hodgetts J, Lomax L, Ashcroft L, Thatcher N and Middleton MR (2003) Randomized phase II study of temozolomide given every 8 hours or daily with either interferon alfa-2b or thalidomide in metastatic malignant melanoma. *J Clin Oncol* **21**:2551-2557.

Dehdashti AR, Hegi ME, Regli L, Pica A and Stupp R (2006) New trends in the medical management of glioblastoma multiforme: the role of temozolomide chemotherapy. *Neurosurg Focus* **20**:E6.

Denny BJ, Wheelhouse RT, Stevens MF, Tsang LL and Slack JA (1994) NMR and molecular modeling investigation of the mechanism of activation of the antitumor drug temozolomide and its interaction with DNA. *Biochemistry* **33**:9045-9051.

Fadnes HO, Reed RK and Aukland K (1977) Interstitial fluid pressure in rats measured with a modified wick technique. *Microvasc Res* **14**:27–36.

Freireich EJ, Gehan EA, Rall DP, Schmidt LH and Skipper HE (1966) Quantitative comparison of toxicity of anticancer agents in mouse, rat, hamster, dog, monkey, and man. *Cancer Chemother Rep* **50**:219-244.

Gallo JM, Vicini P, Orlansky A, Li S, Zhou F, Ma J, Pulfer S, Bookman MA and Guo P (2004) Pharmacokinetic model-predicted anticancer drug concentrations in human tumors. *Clin Cancer Res* **10**:8048-8058.

Gasparini G (2001) Metronomic scheduling: the future of chemotherapy? *Lancet Oncol* **2**:733-740.

Hahnfeldt P, Folkman J and Hlatky L (2003) Minimizing long-term tumor burden: the logic for metronomic chemotherapeutic dosing and its antiangiogenic basis. *J Theor Biol* **220**:545-554.

Jain RK (1987) Transport of molecules in the tumor interstitium: a review. *Cancer Res* **47**:3039–3051.

Jain RK (2005) Normalization of tumor vasculature: an emerging concept in antiangiogenic therapy. *Science* **307**:58-62.

Kato T, Sato K, Kakinuma H and Matsuda Y (1994) Enhanced suppression of tumor growth by combination of angiogenesis inhibitor O-(chloroacetyl-carbamoyl)fumagillol (TNP-470) and cytotoxic agents in mice. *Cancer Res* **54**:5143-5147.

Kerbel RS and Kamen BA (2004) The anti-angiogenic basis of metronomic chemotherapy. *Nat Rev Cancer* **4**:423-436.

Kim JT, Kim JS, Ko KW, Kong DS, Kang CM, Kim MH, Son MJ, Song HS, Shin HJ, Lee DS, Eoh W and Nam DH (2006) Metronomic treatment of temozolomide inhibits tumor cell growth through reduction of angiogenesis and augmentation of apoptosis in orthotopic models of gliomas. *Oncol Rep* **16**:33-39.

Klement G, Baruchel S, Rak J, Man S, Clark K, Hicklin DJ, Bohlen P and Kerbel RS (2000) Continuous low-dose therapy with vinblastine and VEGF receptor-2 antibody induces sustained tumor regression without overt toxicity. *J Clin* Invest **105**:R15-24.

Klink T, Bela C, Stoelting S, Peters SO, Broll R and Wagner T (2006) Metronomic trofosfamide inhibits progression of human lung cancer xenografts by exerting anti-angiogenic effects. *J Cancer Res Clin Oncol* **132**:643-652.

Kurzen H, Schmitt S, Naher H and Mohler T (2003) Inhibition of angiogenesis by non-toxic doses of temozolomide. *Anticancer Drugs* **14**:515-522.

Le QT, Denko NC and Giaccia AJ (2004) Hypoxic gene expression and metastasis. *Cancer Metastasis Rev* **23**:293-310.

Ma J, Fei ZL, Klein-Szanto A and Gallo JM (1998) Modulation of angiogenesis by human glioma xenograft models that differentially express vascular endothelial growth factor. *Clin Exp Metastasis* **16**:559-568.

Ma J, Pulfer S, Li S, Chu J, Reed K and Gallo JM (2001) Pharmacodynamic-mediated reduction of temozolomide tumor concentrations by the angiogenesis inhibitor TNP-470. *Cancer Res* **61**:5491-5498.

Ma J, Li S, Reed K, Guo P and Gallo JM (2003) Pharmacodynamic-mediated effects of the angiogenesis inhibitor SU5416 on the tumor disposition of temozolomide in subcutaneous and intracerebral glioma xenograft models. *J Pharmacol Exp Ther* **305**: 833-839.

Miller KD, Sweeney CJ and Sledge GW Jr (2001) Redefining the target: chemotherapeutics as antiangiogenics. *J Clin Oncol* **19**:1195-1206.

Newlands ES, Blackledge GR, Slack JA, Rustin GJ, Smith DB, Stuart NS, Quarterman CP, Hoffman R, Stevens MF and Brampton MH (1992) Phase I trial of temozolomide (CCRG 81045: M&B 39831: NSC 362856). *Br J Cancer* **65**:287-291.

Nieder C, Grosu AL and Molls M (2000) A comparison of treatment results for recurrent malignant gliomas. *Cancer Treat Rev* **26**:397-409.

Roos WP, Batista LF, Naumann SC, Wick W, Weller M, Menck CF and Kaina B (2007) Apoptosis in malignant glioma cells triggered by the temozolomide-induced DNA lesion O(6)-methylguanine. *Oncogene* **26**:186-197.

Seymour LW (1992) Passive tumor targeting of soluble macromolecules and drug conjugates. *Crit Rev Ther Drug Carrier Syst* **9**:135-187.

Shaked Y, Emmenegger U, Francia G, Chen L, Lee CR, Man S, Paraghamian A, Ben-David Y and Kerbel RS (2005) Low-dose metronomic combined with intermittent bolus-dose

cyclophosphamide is an effective long-term chemotherapy treatment strategy. *Cancer Res* **65**:7045-7051.

Stevens MF, Hickman JA, Langdon SP, Chubb D, Vickers L, Stone R, Baig G, Goddard C, Gibson NW and Slack JA (1987) Antitumor activity and pharmacokinetics in mice of 8-carbamoyl-3-methyl-imidazo[5,1-d]-1,2,3,5-tetrazin-4(3H)-one (CCRG 81045; M & B 39831), a novel drug with potential as an alternative to dacarbazine. *Cancer Res* **47**:5846-5852.

Surawicz TS, Davis F, Freels S, Laws ER, Jr. and Menck HR (1998) Brain tumor survival: results from the National Cancer Data Base. *J Neuro-oncol* **40**:151-160.

Tosoni A, Cavallo G, Ermani M, Scopece L, Franceschi E, Ghimenton C, Gardiman M, Pasetto L, Blatt V and Brandes AA (2006) Is protracted low-dose temozolomide feasible in glioma patients? *Neurology* **66**:427-429.

Trivedi RN, Almeida KH, Fornsaglio JL, Schamus S and Sobol RW (2005) The role of base excision repair in the sensitivity and resistance to temozolomide-mediated cell death. *Cancer Res* **65**:6394-6400.

Tuettenberg J, Grobholz R, Korn T, Wenz F, Erber R and Vajkoczy P (2005) Continuous low-dose chemotherapy plus inhibition of cyclooxygenase-2 as an antiangiogenic therapy of glioblastoma multiforme. *J Cancer Res Clin Oncol* **131**:31-40.

Vaupel P, Kallinowski F and Okunieff P (1989) Blood flow, oxygen and nutrient supply, and metabolic microenvironment of human tumors: a review. *Cancer Res* **49**:6449-6465.

Wang Y, Wong SL and Sawchuk RJ (1993) Microdialysis calibration using retrodialysis and zero-net flux: application to a study of the distribution of zidovudine to rabbit cerebrospinal fluid and thalamus. *Pharm Res* **10**:1411-1419.

Footnotes

This work was supported by NIH grants CA72937 and CA85577 to JMG.

Reprint requests should be sent to: James M Gallo, Department of Pharmaceutical Sciences, School of Pharmacy, Temple University, 3307 North Broad Street, Philadelphia, PA 19140. E-mail: jmgallo@temple.edu

Legends for figures.

Fig. 1. Schematic presentation of the PK model containing a 2-compartment plasma disposition model and 1-compartment tumor model. Model parameters include the volume of distribution of the plasma compartment (V_p), the elimination rate constant (K_e), and the intercompartmental rate constants for unbound TMZ (i.e., K_{pt} and K_{tp}). The unbound fraction of TMZ in plasma (f_u) is 0.8 (Gallo et al., 2004). The volume of the tumor compartment (V_t) was fixed at the actual tumor volume measured in individual animals on the day of PK sampling. *The 2-compartment model is shown for the plasma compartment, yet some animals were best-characterized by a 1-compartment model.

Fig. 2. Effect of TMZ (**A**) and PAC (**B**) on *in vitro* proliferation of HUVECs and SF188V+ cells. IC_{50} values are means ± SD of three separate experiments performed in quadruplicate. **P< 0.01 comparing with the 24-h treatment using the equal-variance *t*-test; $^{++}P < 0.01$ comparing with the SF188V+ human glioma cell line using the equal-variance *t*-test.

Fig. 3. Mean TMZ plasma (**A**) and tumor IF (**B**) concentration-time profiles on the 1st day (closed symbols) and the last day (open symbols) of the treatment from both CD (triangles) and MD (squares) groups. Representative model-predicted (—) and observed TMZ plasma (closed squares) and tumor IF (open triangles) concentrations in two SF188V+ tumor-bearing rats receiving TMZ 18 mg/kg/d (**C**) and 3.23 mg/kg/d (**D**), respectively. *Bars*, SD.

Fig. 4. The effect of different TMZ dosing regimens on (**A**) tumor growth, (**B**) tumor interstitial fluid pressure, and (**C**) tumor pH in nude rats bearing SF188 V+ xenografts. SF188 V+ cells (5×10^6) were injected subcutaneously and treatment was initiated when xenografts reached about 1.0 cm^3. (**A**): **P < 0.01 comparing with the control group. $^{++}P < 0.01$ comparing with day 0. (**B**) and (**C**): $^{\#}P < 0.05$ comparing with the basal level; *P < 0.05, **P< 0.01 comparing with the

central region of the tumor in the control group; $^{+}P < 0.05$, $^{++}P < 0.01$ comparing with the peripheral region of the tumor in the control group. *Bars*, SD.

Fig. 5. Scatterplots of the *HIF-1α* gene expression increase with the *VEGF* gene expression in SF188V+ tumors obtained from (**A**) control group, (**B**) conventional TMZ treatment group and (**C**) metronomic TMZ treatment group. There was a significant correlation between *HIF-1α* and *VEGF* gene expression in all three groups.

Fig. 6. Effect of CD and MD TMZ treatments on the expression of VEGF and HIF-1α in SF188V+ tumors. Semi-quantitative Western blot analysis was performed using tumor samples excised 5, 14 and 28 days after the initiation of the CD or MD TMZ treatment. (**A**). Representative blots of VEGF and HIF-1α with the respective blotting for β-actin used for loading control. (**B** – **C**). Quantification results were expressed as fold changes compared with non-treated control values, and represented as the mean ± S.D. (*N*= 5~6). *P < 0.05, **P < 0.01 comparing with the control group; $^{§}P < 0.05$ comparing with the conventional group; $^{+}P < 0.05$ comparing with the same treatment group on day 5; $^{\#}P < 0.05$, $^{\#\#}P < 0.01$ comparing with the same treatment group on day 14. *Bars*, SD.

JPET Fast Forward. Published on January 26, 2007 as DOI: 10.1124/jpet.106.118265
This article has not been copyedited and formatted. The final version may differ from this version.

Table 1. PK parameters (mean ± SD) of TMZ in plasma and tumor IF in SF188V+ tumor-bearing athymic rats receiving multiple IV administrations of TMZ at a dose level of either 18 mg/kg (the CD regimen) or 3.24 mg/kg (the MD regimen)

Parameters	**CD (*N* = 7)**		**MD (*N* = 9)**	
	Day 1	**Day 5**	**Day 1**	**Day 28**
Plasma				
$C_{max,\,p}$ (μg/mL)	24.1 ± 3.7	21.6 ± 3.2	3.17 ± 0.26	3.33 ± 0.54
$AUC_{0\rightarrow\infty,\,p}$ (μg·h/mL)	24.1 ± 2.6	25.0 ± 5.7	4.27 ± 1.45	3.72 ± 0.89
V_p (L/kg)	0.91 ± 0.30	0.98 ± 0.44	1.14 ± 0.18	1.18 ± 0.41
CL_p (L/h/kg)	0.73 ± 0.11	0.75 ± 0.15	0.85 ± 0.22	0.92 ± 0.21
K_e (h^{-1})	0.87 ± 0.26	0.86 ± 0.29	0.75 ± 0.16	0.81 ± 0.12
$t_{1/2}$ (h)	0.85 ± 0.20	0.89 ± 0.28	0.97 ± 0.27	0.87 ± 0.13
Tumor IF				
$C_{max,\,t}$ (μg/mL)	10.6 ± 3.6	11.1 ± 5.9	4.85 ± 4.08	2.03 ± 0.58
$t_{max,\,t}$ (h)	0.51 ± 0.21	0.77 ± 0.22	0.44 ± 0.23	0.45 ± 0.34
$AUC_{0\rightarrow\infty,\,t}$ (μg·h/mL)	21.0 ± 5.4	31.7 ± 15.1	6.59 ± 4.16	4.55 ± 2.56
V_t (mL)	1.22 ± 0.30	1.33 ± 0.32	1.13 ± 0.20	1.41 ± 0.61
$AUC_{0\rightarrow\infty}$ ratio				
AUC_{tumor} /AUC_{plasma}	0.90 ± 0.35	1.22 ± 0.49	1.56 ± 1.01	1.31 ± 0.84
Intercompartmental rate constant				
K_{pt} (h^{-1})	4.30 ± 5.00	2.69 ± 1.30	6.68 ± 7.50	6.77 ± 3.21**
K_{tp} (h^{-1})	3.02 ± 2.28	1.88 ± 1.47	5.01 ± 3.96	5.13 ± 5.07

**P < 0.01 comparing with the CD group on day 5 using Wilcoxon rank-sum test.

JPET Fast Forward. Published on January 26, 2007 as DOI: 10.1124/jpet.106.118265
This article has not been copyedited and formatted. The final version may differ from this version.

Table 2. Effect of conventional and metronomic TMZ treatment on relative mRNA expression levels of *VEGF*, *HIF-1α*, *TSP-1*, *Ang-1*, *Ang-2* and *Tie-2* in SF188V+ tumors ($N = 7 \sim 8$)

Gene/	**Gene expression median (range)**		
Treatment group	**Day 5**	**Day 14**	**Day 28**
VEGF			
Control	2.18 (1.29 – 46.97)	14.56 (12.88 – 48.96)	7.98 (3.04 – 34.02)
CD	13.55 (6.95 – 34.63)	21.32 (4.56 – 86.71) *	4.42 (0.78 – 29.91)
MD	9.39 (2.38 – 65.79)	18.20 (3.34 – 86.19) *	3.41 (0.66 – 24.91)
HIF-1a			
Control	4.54 (0.44 – 22.07)	3.08 (0.44 – 5.74)	0.69 (0.48 – 1.44) *$^{+}$
CD	1.96 (1.08 – 4.31)	5.88 (1.10 – 12.48)	0.96 (0.27 – 6.41) $^{+}$
MD	2.06 (0.92 – 10.09)	3.94 (0.28 – 15.60)	0.66 (0.11 – 5.86) $^{+}$

*$P < 0.05$ comparing with the same treatment group on day 5 using Wilcoxon rank-sum test; $^{+}P < 0.05$ comparing the same treatment group on day 14 using Wilcoxon rank-sum test.

Fig. 1

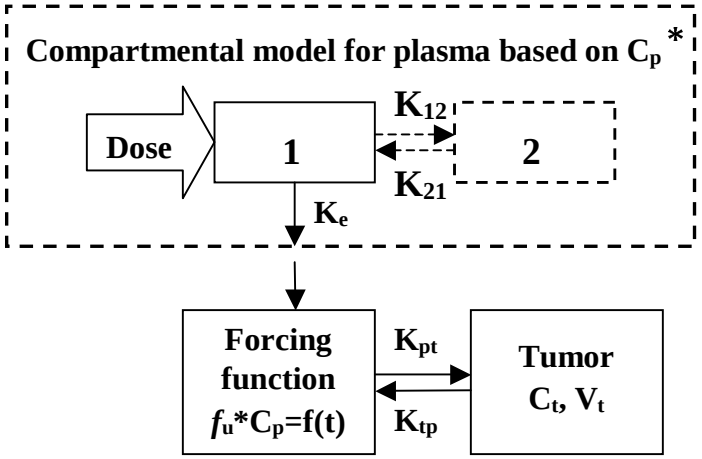

Fig. 2

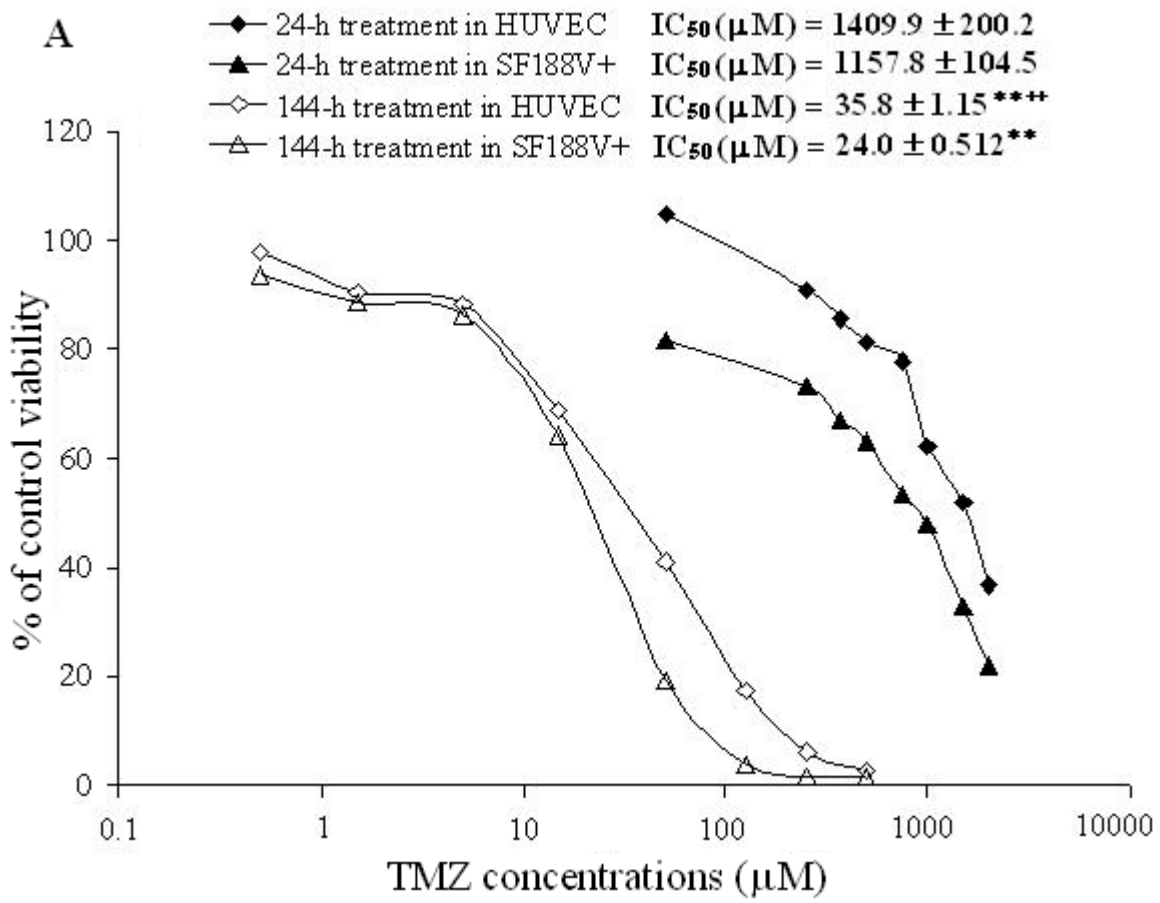

Fig. 2

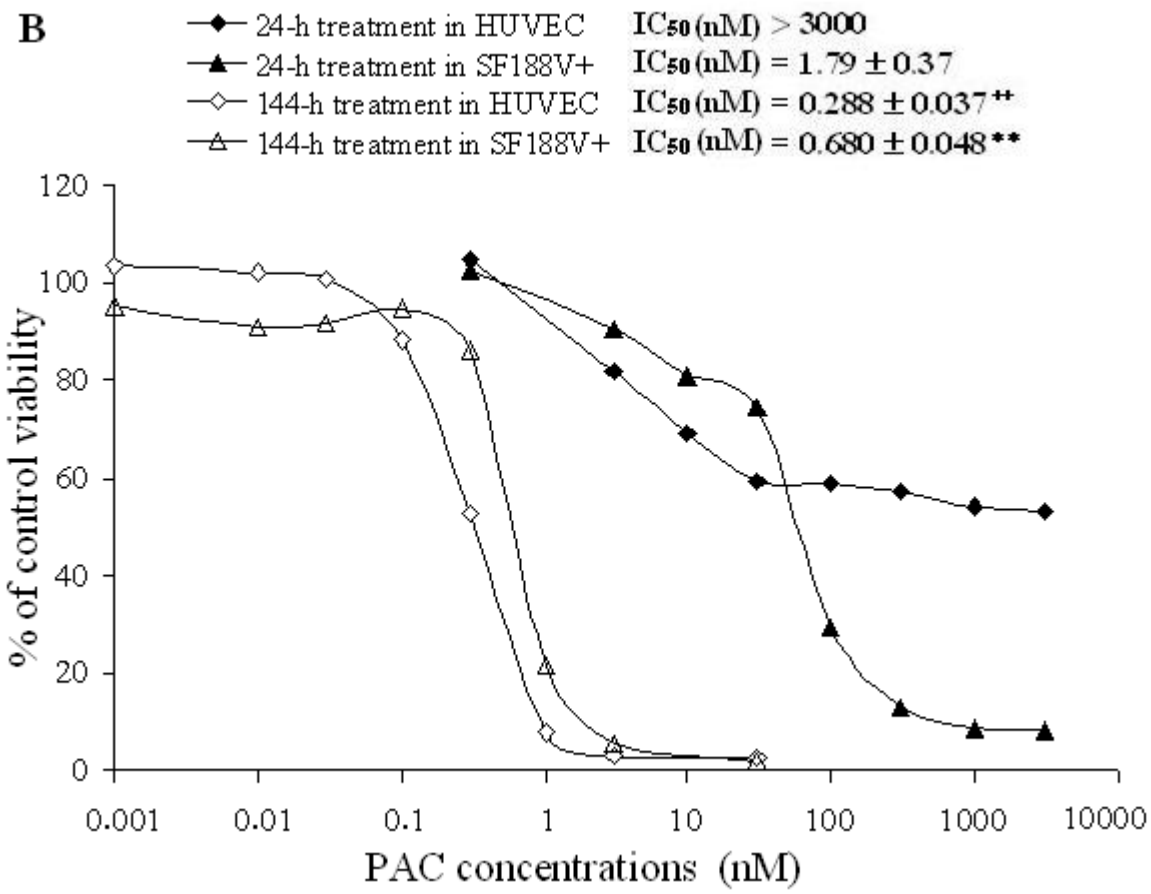

Fig. 3.

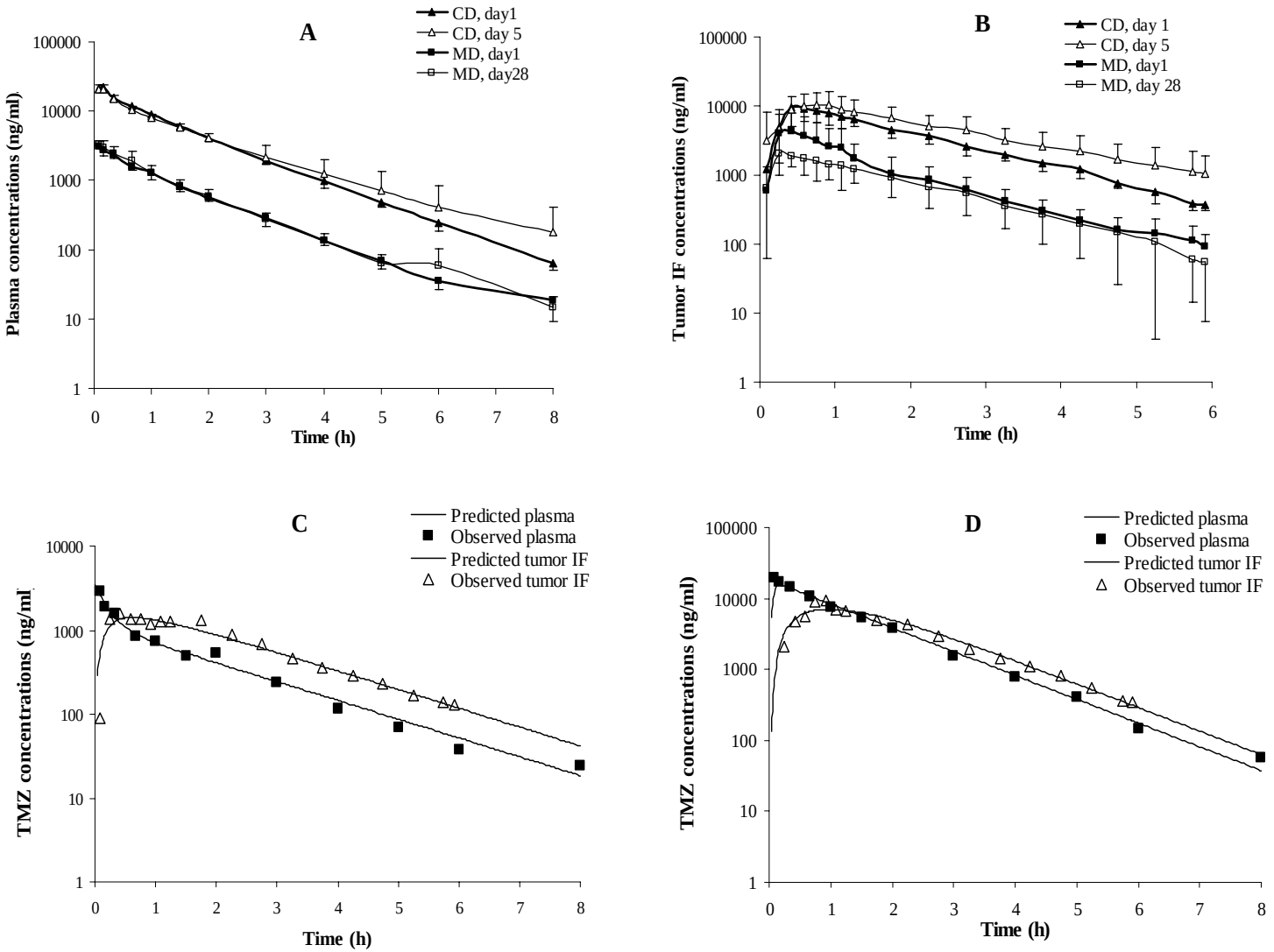

Fig. 4

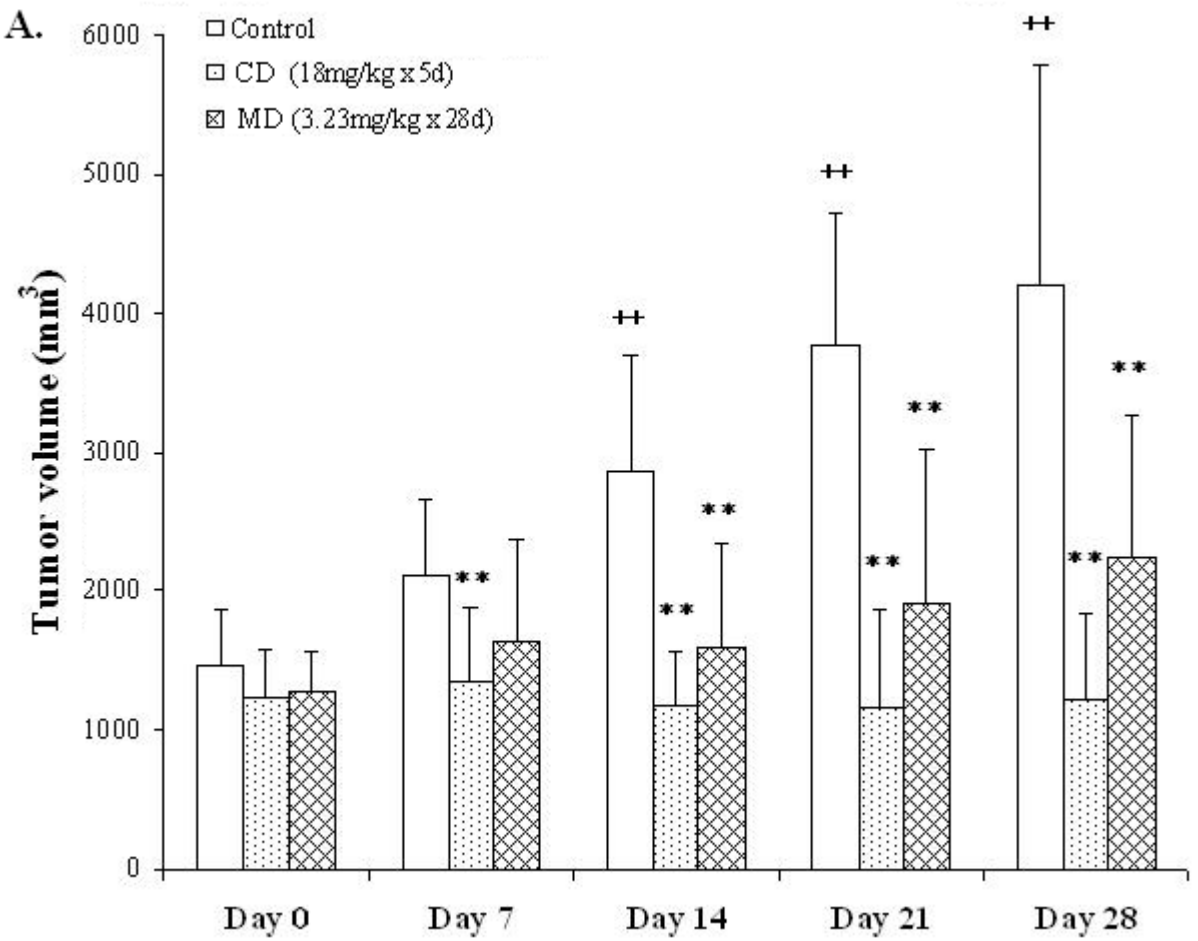

Fig. 4

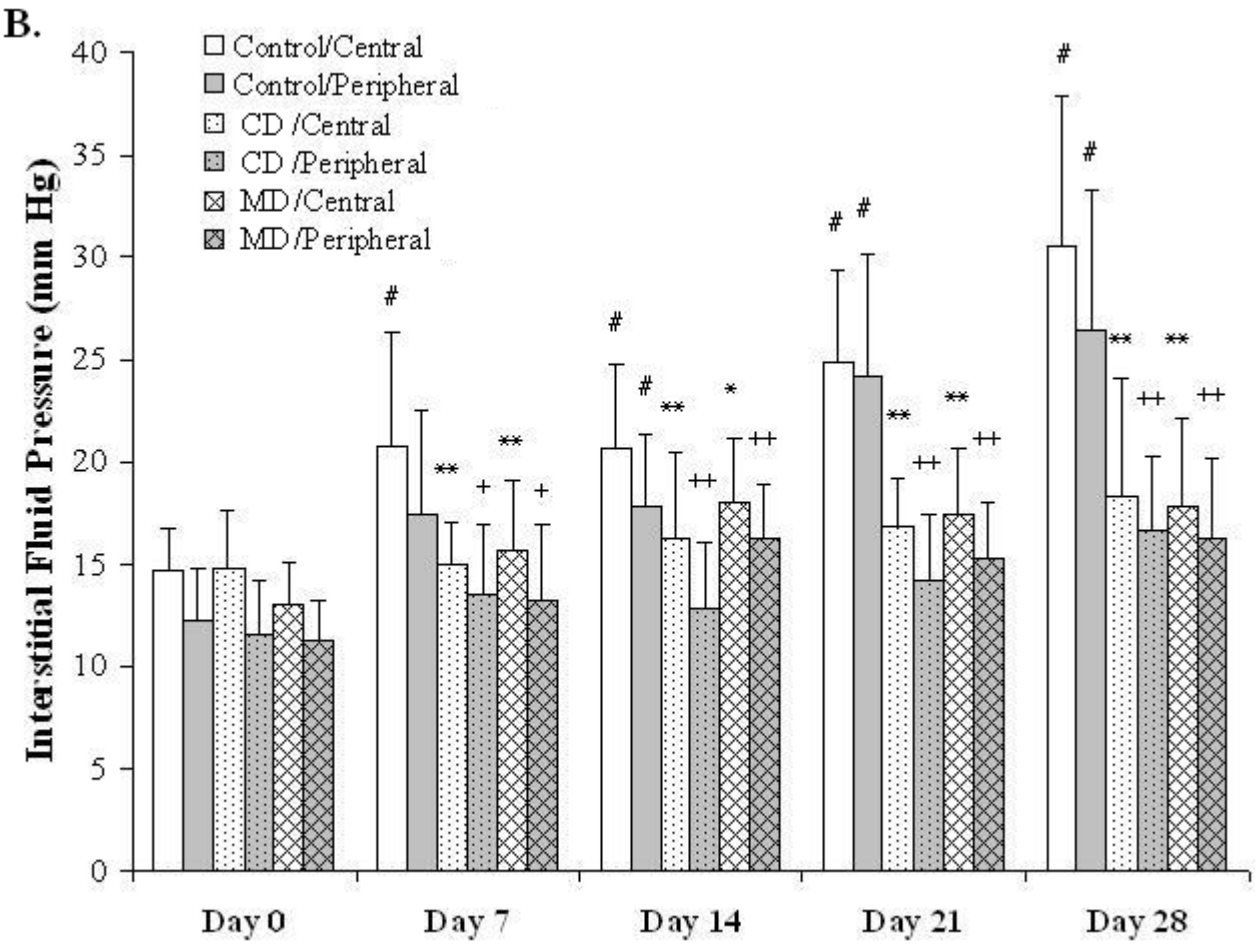

Fig. 4

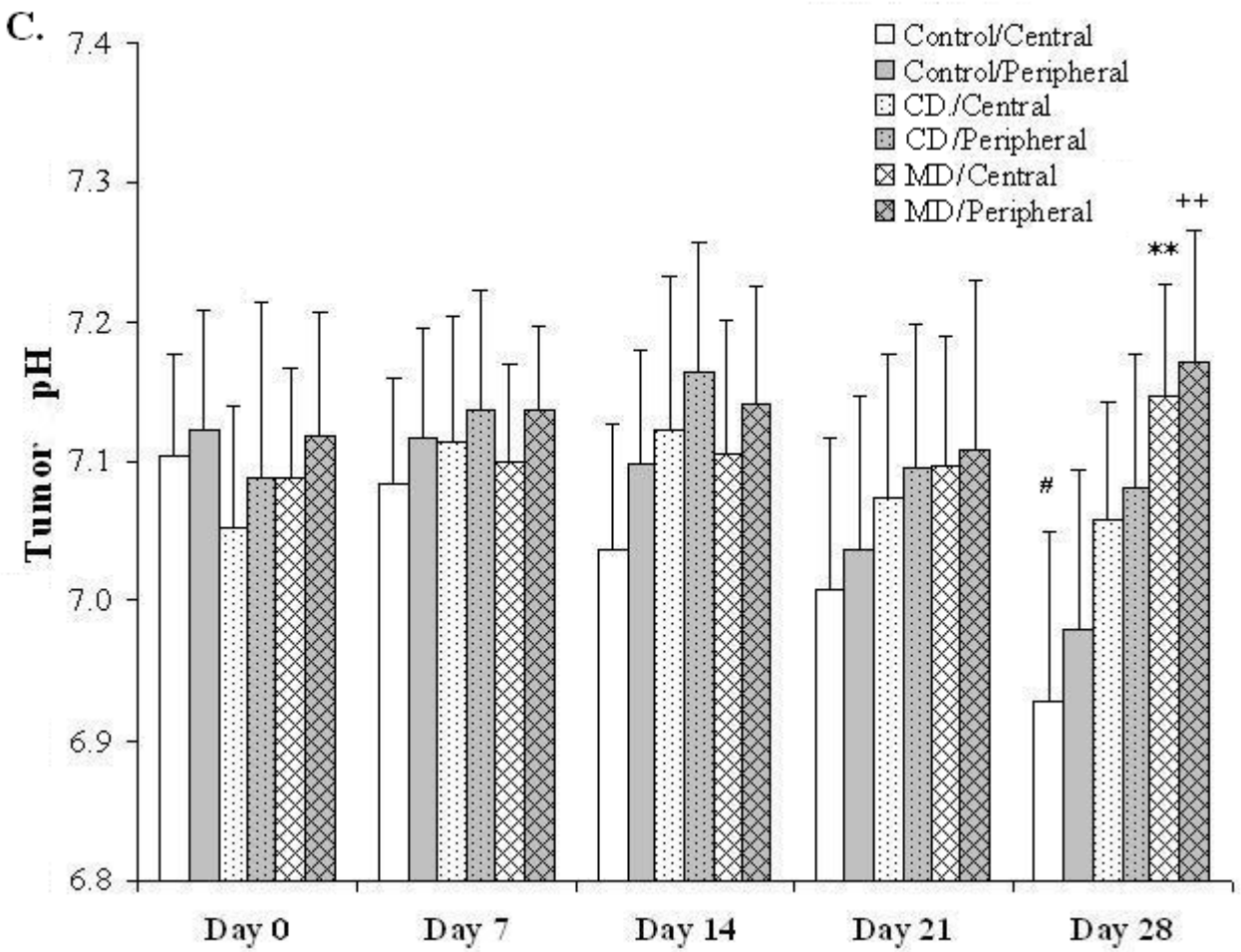

Fig. 5.

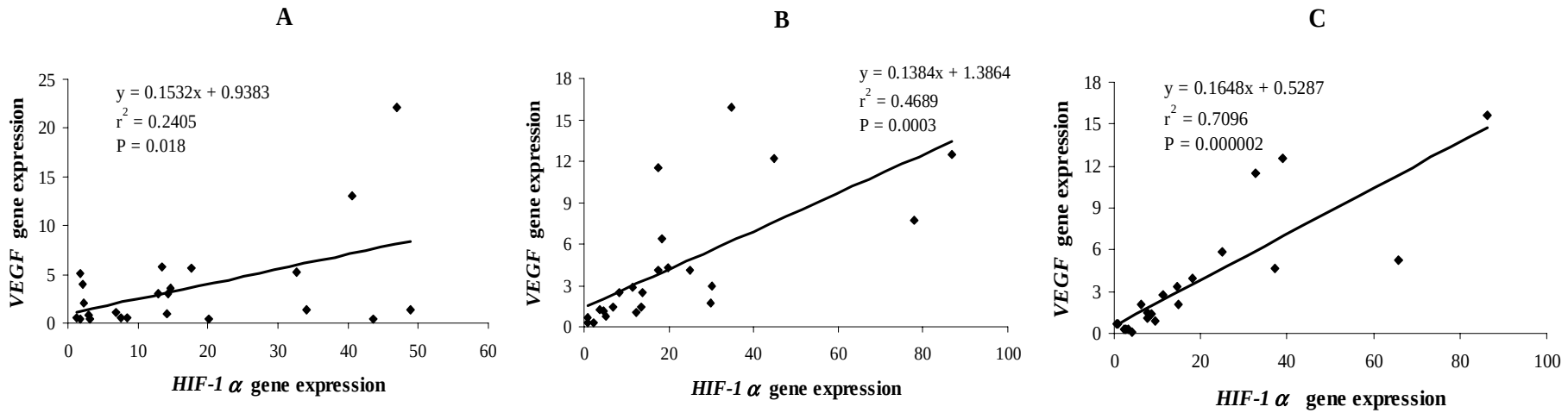

Fig. 6

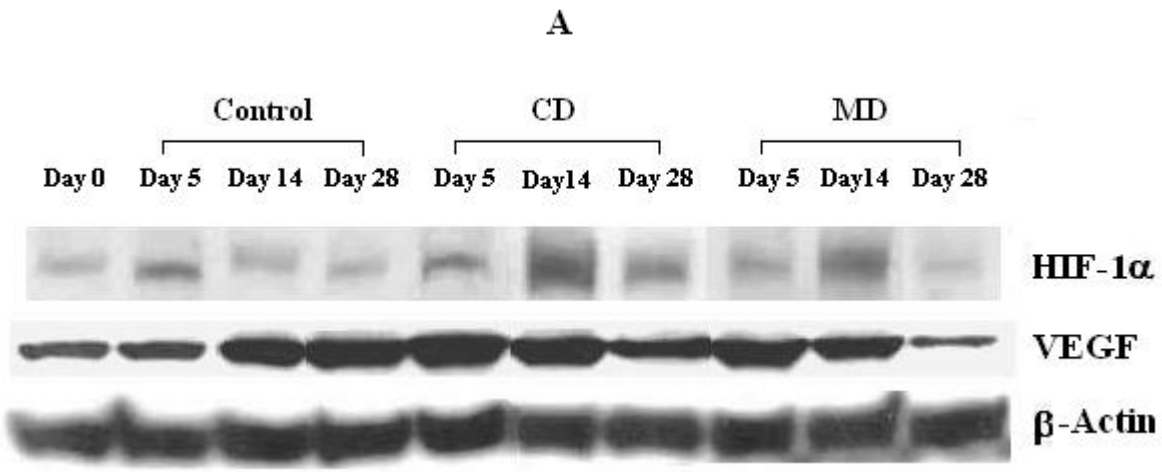

Fig. 6